Smad1, β-catenin and Tcf4 associate in a molecular complex with the Myc promoter in dysplastic renal tissue and cooperate to control Myc transcription

Ming Chang Hu[1] and Norman D. Rosenblum[2,*]

[1]Program in Developmental Biology, Research Institute, The Hospital for Sick Children, 555 University Avenue, Toronto, Ontario M5G 1X8, Canada
[2]Program in Developmental Biology, Research Institute, The Hospital for Sick Children and Division of Nephrology, Department of Paediatrics, University of Toronto, 555 University Avenue, Toronto, Ontario M5G 1X8, Canada
*Author for correspondence (e-mail: norman.rosenblum@sickkids.ca)

Accepted 3 November 2004

Development 132, 215-225
Published by The Company of Biologists 2005
doi:10.1242/dev.01573

Summary

Renal dysplasia, the major cause of childhood renal failure in humans, arises from perturbed renal morphogenesis and molecular signaling during embryogenesis. Recently, we discovered induction of molecular crosstalk between Smad1 and β-catenin in the *TgAlk3^{QD}* mouse model of renal medullary cystic dysplasia. Our finding that Myc, a Smad and β-catenin transcriptional target and effector of renal epithelial dedifferentiation, is misexpressed in dedifferentiated epithelial tubules provided a basis for investigating coordinate transcriptional control by Smad1 and β-catenin in disease. Here, we report enhanced interactions between a molecular complex consisting of Smad1, β-catenin and Tcf4 and adjacent Tcf- and Smad-binding regions located within the Myc promoter in *TgAlk3^{QD}* dysplastic renal tissue, and Bmp-dependent cooperative control of Myc transcription by Smad1, β-catenin and Tcf4. Analysis of nuclear extracts derived from *TgAlk3^{QD}* and wild-type renal tissue revealed increased levels of Smad1/β-catenin molecular complexes, and de novo formation of chromatin-associated Tcf4/Smad1 molecular complexes in *TgAlk3^{QD}* tissues. Analysis of a 476 nucleotide segment of the 1490 nucleotide Myc genomic region upstream of the transcription start site demonstrated interactions between Tcf4 and the Smad consensus binding region and associations of Smad1, β-catenin and Tcf4 with oligo-duplexes that encode the adjacent Tcf- and Smad-binding elements only in *TgAlk3^{QD}* tissues. In collecting duct cells that express luciferase under the control of the 1490 nucleotide Myc genomic region, Bmp2-dependent stimulation of Myc transcription was dependent on contributions by each of Tcf4, β-catenin and Smad1. These results provide novel insights into mechanisms by which interacting signaling pathways control transcription during the genesis of renal dysplasia.

Key words: Smad1, β-catenin, Tcf4, renal dysplasia, cystogenesis, Myc

Introduction

Renal dysplasia, a polymorphic disorder defined as malformation of renal tissue elements, is the major cause of renal failure during childhood (Neu et al., 2002). Although the molecular etiology of renal dysplasia is largely unknown, new knowledge regarding the molecular control of normal renal development is providing an expanding conceptual basis for the discovery of pathogenic mechanisms (Pohl et al., 2002). Normal kidney development is dependent on inductive interactions between the metanephric blastema, a mesenchymal tissue, and the ureteric bud, an epithelial structure (Saxen, 1987). In response to secreted signals elaborated by each of these tissue elements, the ureteric bud invades the metanephric blastema at 5 weeks gestation in the human and E10.5 in the mouse. Cells of the metanephric blastema adjacent to the tip of the ureteric bud are induced to undergo a mesenchymal-epithelial transformation which results in formation of all epithelial structures (glomerulus, proximal and distal tubules, loop of Henle) other than the collecting ducts. In reciprocal fashion, the ureteric bud is induced to grow and branch, a process known as branching morphogenesis. Ureteric bud branches differentiate into collecting ducts that, starting at ~E15.5, are organized geographically into the cortex and medulla of the kidney during the stage of cortico-medullary patterning. Disruption of the normal morphological development of any of these epithelial structures and attendant patterning events can generate a dysplastic phenotype characterized in humans by variable degrees of abnormal mesenchymal and epithelial differentiation and epithelial cyst formation.

The stereotypic pattern of kidney development suggests that the morphogenetic pathways that regulate renal formation are tightly regulated. Indeed, investigation of the signaling pathways that control renal branching morphogenesis has demonstrated the existence of pathways that stimulate or inhibit epithelial tubule growth and branching in a coordinated manner (Piscione and Rosenblum, 2002). Members of the bone morphogenetic protein (Bmp) family inhibit ureteric bud growth and branching in in vitro models of branching

morphogenesis and in vivo (Hu et al., 2003; Miyazaki et al., 2000; Piscione et al., 1997). Recently, we have described a novel model of renal medullary cystic dysplasia in *TgAlk3^{QD}* mice, while investigating the functions of the bone morphogenetic protein cell surface receptor, activin-like kinase (Alk) 3, during renal embryogenesis (Hu et al., 2003). *Alk3* is expressed in both the metanephric mesenchyme and the ureteric bud during the early stages of kidney development and at lower levels towards the end of gestation (Dewulf et al., 1995). In *TgAlk3^{QD}* mice, overexpression of a constitutive active form of Alk3 (Alk3^{QD}) in the ureteric bud lineage inhibits branching morphogenesis during the early stages of renal development and causes cystic malformation of medullary collecting ducts later in utero during the stage of cortico-medullary patterning. The epithelial cells that populate collecting duct cysts are remarkable for loss of E-cadherin, a marker of epithelial cell differentiation, increased cell proliferation and expression of the proto-oncogene Myc. As inhibition of aberrant Myc expression in a model of polycystic kidney disease ameliorates the cystic phenotype (Ricker et al., 2002), discovery of molecular mechanisms that control Myc expression is likely to provide insights into epithelial cell differentiation in normal and dysplastic tissues.

Our investigations of pathogenic mechanisms controlling the formation of a dysplastic kidney in *TgAlk3^{QD}* mice led us to discover a marked increase in the expression of β-catenin, an intracellular effector in the Wnt signaling pathway, in the medulla of dysplastic kidney tissue. Moreover, we identified molecular interactions between β-catenin and Smad1, an intracellular effector of Bmp-Alk signaling in *TgAlk3^{QD}* kidney tissue. The presence of consensus binding sequences for both Smads and Tcfs, transcription partners for β-catenin, in the Myc promoter led us to hypothesize that Smad1 and β-catenin, together with its Tcf partners, interact to control Myc and epithelial cell differentiation. Here, we investigated these interactions within a 1490 nucleotide segment of the Myc promoter that contains adjacent regions containing a cluster of Tcf and Smad consensus binding sequences. Our analysis of renal tissue derived from *TgAlk3^{QD}* and wild-type mice demonstrate increased levels of Smad1/β-catenin/Tcf4 molecular complexes and novel associations between these effectors and the Myc promoter in dysplastic tissues. Our investigation of the functional significance of these interactions reveals that each of Tcf4, β-catenin and Smad1 are required for Bmp-dependent stimulation of Myc transcription. These results provide novel insights into the significance of crosstalk among signaling pathways during tissue development and, specifically, during the genesis of renal dysplasia.

Materials and methods

TgAlk3^{QD} transgenic mice

TgAlk3^{QD} homozygous mice were generated via injection of human *Alk3^{QD}* cDNA under the control of a *hoxb.7* promoter and bred on a CD1 genetic background (Hu et al., 2003).

Antibodies and Bmp2

Immunohistochemistry (IHC) was performed using paraffin wax-embedded tissue sections (4 μm) generated from adult kidney tissue as described (Hu et al., 2003) with the following antibodies: rabbit anti-phospho-Smad1 (1:10; Cell Signaling, Beverly, MA), mouse anti-Tcf4 (1:10 dilution; Upstate Biotech, Lake Placid, NY), rabbit anti-β-catenin (1:25 dilution; Upstate Biotech, Lake Placid, NY) and mouse anti-β-catenin (1:25 dilution; BD Transduction Laboratories, Mississauga, ON, Canada). Biotinylated secondary antibodies were used in a biotin-avidin complex assay (Vector Laboratories, Burlingame, CA). Immunofluorescence (IF) was performed using anti-mouse or anti-rabbit fluorescein- or rhodamine-conjugated secondary antibodies (Jackson ImmunoResearch Laboratories, Wester Glove, PA). Immunoblotting was performed using anti-Smad1 (1:250 dilution), anti-Tcf4 (1:250 dilution), anti-Smad4 (1:250 dilution), anti-β-catenin (1:250 dilution) anti-β-actin (1:3000 dilution, Sigma, St Louis, MO) and anti-acetyl Histone 4 (1:250 dilution, Upstate) antibodies. Bmp2 was provided by Wyeth as per a material transfer agreement.

Fractionation of cytosolic and nuclear proteins

Cytosolic and nuclear proteins were prepared from P30 kidneys using published methods (Saifudeen et al., 2002). Cytosolic or nuclear proteins (1 mg) were subjected to immunoprecipitation. Proteins (40 μg) were directly subjected to SDS-PAGE and transferred to PVDF membrane.

Identification of proteins associated with chromatin

Proteins associated with chromatin were identified by cisplatin crosslinking (Chichiarelli et al., 2002). Nuclear proteins prepared from a single P30 kidney were added to 10 ml of 1 mM cis-diammineplatinum (II) dichloride (cisplatin) (Sigma, Saint Louis, MO) and then incubated at 37°C for 2 hours while rotating. The protein pellet was washed with 5 mM thiourea for 5 minutes at room temperature to inactivate free cisplatin. Pellets were resuspended in 5 ml of nuclear lysis buffer at 4°C for 30 minutes. The crosslinked sample (4 mg) was mixed with 1 g of pre-equilibrated hydroxyapatite resin (HTP) (DNA grade bio-gel HTP, BioRad, CA) at 4°C for 1 hour. After centrifugation, the precipitated mixture was washed twice with lysis buffer to remove free protein. To release the protein from chromatin, 5 ml of reverse buffer was incubated with the HTP resin pellet overnight at 4°C. After centrifugation, the supernatant was dialyzed against distilled water for 24 hours at 4°C (Spectra/Por #2, MW cutoff 12,000~14,000, Spectrum Medical Industries, Houston, TX). The dialyzed solution was concentrated using a Centricon YM-10 filter (Millipore Corporation, Bedford, MA). The retained solution was stored at –70°C.

Chromatin immunoprecipitation

Chromatin immunoprecipitation (ChIP) was performed using commercially available reagents (Upstate Biotech) and published modifications (Weinmann and Farnham, 2002). Briefly, nuclear extracts were treated with formaldehyde (1% final concentration) to crosslink proteins to DNA. The reaction was stopped by the addition of 125 mM glycine. Soluble chromatin with an average size of ~200-500 bp was prepared by sonication (Weinmann et al., 2001). After immunoprecipitation, molecular complexes consisting of chromatin, protein and antibody were precipitated with a pre-prepared mixture of Salmon sperm DNA and protein A agarose (Upstate), and then lysed with 1% SDS in 0.1 M $NaHCO_3$. Proteinase K was added to digest protein in complexes. Supernatants were used for PCR. The 185 bp TBE-A region (–1322 to –1160) (Fig. 3) was amplified using primers: sense, 5′-CAAGCTTTAATTAGCTTAACACA-3′; anti-sense, 5′-GGAGCCTGCAGAGACCCTA-3′ at an annealing temperature of 52°C for 30 seconds. The 229 bp SBE-A region (–1056 to –946) was amplified using primers: sense, 5′-CGCGTCTAGCCTTGATTTTC-3′; anti-sense, 5′-GGCTCTTTCCCCCTGTAGGTC-3′ at an annealing temperature of 52°C for 30 seconds. The 579 bp SBE-B region (–572 to –13) was amplified using primers: sense, 5′-GCA-ATTTTAATAAAATTCCAGACA-3′; anti-sense, 5′-AGACCCC-CGGAATATAAAGG-3′ at an annealing temperature of 54°C for 30 seconds. The 104 bp RNA polymerase II core promoter region (–40 to

–24) was amplified using primers: sense, 5′-AAACGAGGAGGAAGGAAA-3′; anti-sense, 5′-GCAGACCCCCCGGAATATAA-3′ at an annealing temperature of 53°C for 40 seconds.

Site-directed mutagenesis

Site-directed mutagenesis of the murine *Myc* promoter was performed using commercially available reagents (Stratagene, La Jolla, CA) to generate the following changes in nucleotide identity: TBE-A, ACTTTG**AT**C to ACTTTG**GC**C; and SBE-A, **AGAC**CGGCAG**AGAC** to **GAGT**CGGCAG**GAGT**. Primers used to generate the mutant TBE encompassed nucleotides –1292 to –1248 (Fig. 3) and consisted of: sense, 5′-GGCAAAAATGTAACGTTACTTTG**GC**CTGATCAGGGCCGACTTTTT-3′; and antisense, 5′-AAAAAGTCGGCCCTGATCAG**GC**CAAAGTAACGTTACATTTTTGCC-3′. Primers used to generate the mutant SBE encompassed nucleotides –939 to –889 and consisted of: sense, 5′-GTGGAGGTGTATGGGGTGT**GAGT**CGGCAG**GAGT**TCCTCCCGGAGGAGCCGG-3′; and antisense, 5′-CCGGCTCCTCCGGGAGGA**ACTC**CTGCCG**ACTC**ACACCCCATACACCTCCAC-3′ (mutant nucleotides shown in bold). The mutated sequences were verified by DNA sequencing.

Electrophoretic mobility gel shift assay

Electrophoretic mobility gel shift assays (EMSA) were performed as described (Saifudeen et al., 2002) with modifications. The following oligonucleotides encoding regions of the mouse Myc promoter were used: a 36 bp oligonucleotide (–1294 to –1258, 5′-GGCAAAAATGTAACGTTACTTTGATCTGATCAGGGC-3′) containing a Tcf consensus sequence (TTTGATCT), a mutant 36 bp oligonucleotide containing mutated Tcf consensus sequence (TTTGGCCT), a 46 bp oligonucleotide (–939 to –893, 5′-GTGGAGGTGTATGGGGTGTAGACCGGCAGAGACTCCTCCCGGAGGAG-3′) containing two Smad-binding sequences (AGAC), and a mutant 46 bp oligonucleotide containing mutant Smad-binding sequences (GAGT). Protein (10 μg) derived from nuclear extract was incubated with ^{32}P-labeled oligonucleotide probes and/or unlabeled probes and in some experiments with 1 μg of anti-Smad1, anti-Tcf4 or anti-β-catenin antibody. The migratory characteristics of the radiolabeled probes were analyzed in 5% non-denaturing polyacrylamide/bisacrylamide gels.

RNA interference

RNAi interference (RNAi) was performed using the pSUPER RNAi system (OligoEngine, Seattle, WA) (Brummelkamp et al., 2002) and synthetic 64 bp double-stranded oligonucleotides designed to encode 19 nucleotide target sequences and their reverse complement separated by a spacer region. Oligonucleotide exact-match sequences (19 mer) corresponding to sequences in β-catenin, Smad1 and Tcf4 were selected based on their respective mRNA sequences (GenBank Accession Numbers: mouse β-catenin, NM007614; mouse Smad1, AH010073; mouse Tcf4, AJ22230770). Based on their efficiency in decreasing endogenous mRNA and protein levels, the following sequences were used: β-catenin, 5′-^{163}GAAGATGTTGAACACCTCCC-3′; Smad1, 5′-^{243}GGGACTACCTCATGTCATT-3′; and Tcf4, 5′-^{1149}CGACAGCTTCACAATGCAGC-3′. Oligonucleotides (64 mer) were annealed and cloned into pSuper at the *Bgl*II and *Hin*dIII sites. Positive clones were identified by DNA sequencing.

Luciferase assay

The mouse *Myc* promoter (–1490 to –1), amplified by PCR, was inserted into a luciferase expression vector upstream of a minimal *Fos* promoter (kindly provided by Dr B. Alman, The Hospital for Sick Children, Toronto, Canada). Transient transfection was performed using Fugene 6 (Roche Diagnostics Corporation, Indianapolis, IN) and *lacZ* as a transfection control. Cell lysates were prepared for a luciferase activity assay using commercial reagents (Promega, Madison, WI). Luminescence was recorded using a Monolight 2010 Luminometer.

Data analysis

Mean differences between groups were examined by Student's *t*-test (two-tailed) or by ANOVA using commercially available software (Statview, version 4.01; Abacus Concepts, Berkeley, CA). Statistical significance was taken at a value of $P<0.05$.

Results

Aberrant Myc expression in the *TgAlk3^{QD}* model of medullary cystic dysplasia

Previously, we have reported a novel model of medullary renal dysplasia in mice expressing a constitutive active Bmp receptor, Alk3^{QD}, in the ureteric bud lineage (Hu et al., 2003). In these mice, expression of Alk3^{QD} in ureteric bud branches and their daughter collecting ducts throughout renal embryogenesis results in medullary cystic dysplasia that is characterized by a decreased number of medullary tubules, loss of epithelial differentiation markers and cystic malformation of epithelial tubules (Fig. 1A). Remarkably, Myc, a proto-oncogene misexpressed in dedifferentiated tubular epithelia in polycystic kidney disease (Cowley et al., 1987), was expressed in a nuclear pattern in cystic tubules in *TgAlk3^{QD}* mice (Fig. 1A). As interruption of Myc expression blocks the development of murine polycystic kidney disease (Ricker et al., 2002), we began to investigate the mechanisms controlling increased Myc expression in *TgAlk3^{QD}* mice. We analyzed Myc promoter activity in dysplastic and normal kidney tissue using the association of acetylated Histone 4 (H4) with the RNA polymerase core promoter as a marker of transcriptional activity (Grunstein, 1997). Nucleotide sequences encoding a TATA box and a TFIIB recognition element (BRE), signature features of a RNA polymerase core promoter, are located at –24 to –40 within the murine Myc promoter (Fig. 1B). We used ChIP to determine the association of acetyl H4 with a 104 nucleotide region encompassing the core promoter in wild-type and *TgAlk3^{QD}* kidney tissues. Our results demonstrate a 1.6-fold increase in the association between acetyl H4 and this region in *TgAlk3^{QD}* dysplastic kidney tissue (Fig. 1B). This result is consistent with enhanced transcriptional activity of the Myc promoter and the aberrant expression of Myc protein in *TgAlk3^{QD}* dysplastic renal tissue.

Molecular associations between Smad1 and β-catenin/Tcf4 in *TgAlk3^{QD}* dysplastic kidney nuclei

Our initial investigations of the mechanisms controlling the dysplastic renal phenotype in *TgAlk3^{QD}* mice revealed a marked cellular elevation of molecular complexes consisting of Smad1 and β-catenin (Hu et al., 2003). This observation was particularly interesting as the Myc promoter contains Smad-binding elements as well as binding elements for Tcfs (Yagi et al., 2002), a family of β-catenin transcriptional partners. Together, these observations suggested that Smad1 and β-catenin may interact to control Myc transcription. Our approach was to identify Tcfs that are expressed in wild-type and *TgAlk3^{QD}* postnatal mouse kidney and then investigate Smad1/β-catenin/Tcf expression and molecular interactions in the nucleus. A survey of Tcfs using specific antisera demonstrated expression of Tcf4 with particularly high levels

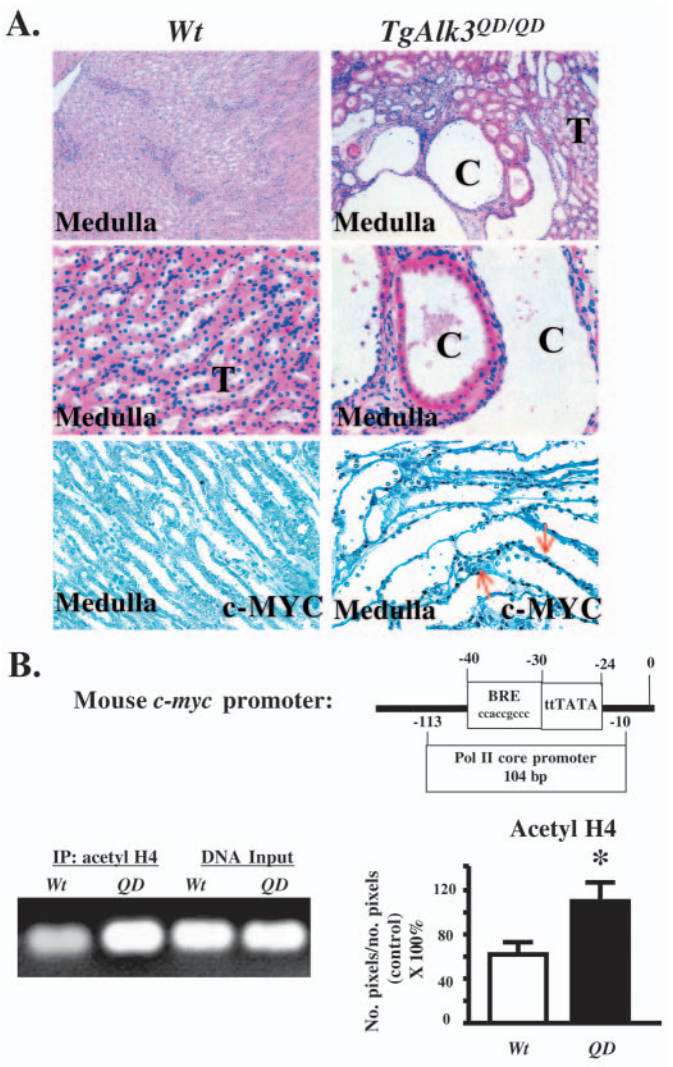

Fig. 1. *TgAlk3*^{QD} mice exhibit medullary cystic renal dysplasia and aberrant Myc expression. (A) Histological phenotype and Myc expression. Histological analysis of 4 μm Hematoxylin and Eosin-stained kidney tissue sections. Upper and middle panels: the renal medulla of wild-type mice is characterized by a high density of closely apposed tubules without intervening extracellular matrix. By contrast, the renal medulla of *TgAlk3*^{QD} mice is characterized by a heterogeneous population of tubules of irregular shape and variable diameter. Cysts (C) with greatly increased diameter and flattened epithelium are contrasted with normal tubules (T). Lower panels: Myc was detected using an anti-Myc antibody. Although Myc was barely detected in wild-type kidney, it was widely expressed in a nuclear pattern in dysplastic renal tubules. (B) Association of acetyl histone 4 (H4) with the RNA polymerase II core promoter using ChIP. The location and characteristics of the RNA polymerase II core promoter including the TATA box and TFII recognition elements (BRE) in the murine *Myc* gene are shown in schematic form. Left lower panel: ChIP using an anti-acetyl-histone 4 (H4) and kidney tissue isolated from wild-type or *TgAlk3*^{QD} kidney tissue demonstrated increased amplification of the 103 nucleotide core promoter region in dysplastic (QD) tissue. Lower right panel: quantitation of DNA amplified after ChIP, demonstrating a 1.6-fold increase in acetyl-H4 association with the core promoter amplified from *TgAlk3*^{QD} tissue. The amount of DNA amplified was controlled for the amount of input DNA. $P<0.05$, $n=3$ independent experiments.

in *TgAlk3*^{QD} kidney. Immunofluorescence imaging of kidney tissue revealed a remarkable difference in the pattern of Smad1, β-catenin and Tcf4 in kidney tissue isolated from *TgAlk3*^{QD} versus wild-type mice (Fig. 2A). Although each of phospho-Smad1 (P-Smad1, the activated from of Smad1), β-catenin and Tcf4 were expressed in a cytoplasmic pattern in wild-type tissue, in *TgAlk3*^{QD} tissue, each was expressed in a nuclear pattern. Moreover, nuclear co-localization of P-Smad1 with Tcf4 and of β-catenin with Tcf4 in *TgAlk3*^{QD} tissue suggested that these effectors interact to control transcription.

We confirmed our results generated by immunofluorescence by performing a biochemical analysis of Smad1/β-catenin/Tcf4 interactions in nuclear extracts generated from wild-type and *TgAlk3*^{QD} kidney tissues (Fig. 2B). Our results demonstrate a 1.9-fold increase in β-catenin/P-Smad1 molecular complexes and a 2.3-fold increase in β-catenin/Tcf4 molecular complexes in the nuclei of *TgAlk3*^{QD} tissue. To determine whether these protein interactions occur in association with chromatin, we performed cisplatin crosslinking on nuclear extracts generated from wild-type and *TgAlk3*^{QD} tissues (Chichiarelli et al., 2002). Consistent with our results in nuclear extracts (Fig. 2B), we detected a threefold increase in molecular complexes consisting of β-catenin and Smad1 associated with chromatin. Remarkably, molecular complexes consisting of Tcf4 and Smad1 associated with chromatin were detected in *TgAlk3*^{QD} tissue but not in wild-type tissue (Fig. 2C). This finding is consistent with our findings derived from immunofluorescence imaging of normal and dysplastic renal tissues (Fig. 2A). Taken together, these experiments demonstrate increased localization of Smad1, β-catenin and Tcf4 in the nuclear compartment of *TgAlk3*^{QD} tissues and interactions between Smad and β-catenin effectors in renal dysplasia.

Smad1, β-catenin and Tcf4 interact with Smad and Tcf binding elements in the Myc promoter

Smad and β-catenin/Tcf consensus binding sites have been identified previously in the murine Myc promoter (He et al., 1998; Yagi et al., 2002). Inspection of the 1500 nucleotide sequence upstream of the transcription start site (GenBank M12345) reveals that Tcf and Smad consensus binding elements are organized in groups in three discrete regions (Fig. 3A). We designated these regions TBE (Tcf-binding region)-A, SBE (Smad-binding region)-A and SBE-B. The geographic organization of these elements, specifically TBE-A and SBE-A, in close proximity to each other, provided a basis for examining Smad1/β-catenin/Tcf4 interactions at this promoter. First, we determined the association of these proteins with their respective binding regions using ChIP and specific antibodies (Fig. 3B). The association of Tcf4 with TBE-A was increased 4.7-fold in *TgAlk3*^{QD} kidney tissue. Similarly, the association of Smad1 with each of SBE-A and SBE-B was increased 2.6-fold. Having demonstrated associations between Tcf4 and Smad1, we used ChIP to determine whether Tcf4 interacts with the SBE (SBE-A) adjacent to TBE-A. Indeed, after immunoprecipitation of proteins crosslinked to DNA using anti-Tcf4 antibody, we were able to amplify SBE-A. Moreover, amplification of SBE-A was detected only in *TgAlk3*^{QD} tissue, consistent with our detection in *TgAlk3*^{QD} tissue, but not in wild-type tissue, of Tcf4/Smad1 protein associations (Fig. 2C). The specificity of the interaction of Tcf4 with SBE-A was

demonstrated by a failure to amplify the more distant SBE-B region in experiments conducted in parallel.

Our results using ChIP, together with those using immunoprecipitation and immunoblotting of nuclear extracts, suggested that Smad1 and β-catenin/Tcf4 associate in a molecular complex at the Myc promoter region encoding Tcf-A and SBE-A. We tested this possibility using EMSA and oligonucleotide duplexes encoding the Tcf consensus binding sequences within TBE-A and the Smad consensus binding sequences within SBE-A (Fig. 4). The migration of a radiolabeled oligo-duplex encoding a 36 nucleotide sequence within TBE-A was retarded by nuclear extract prepared from

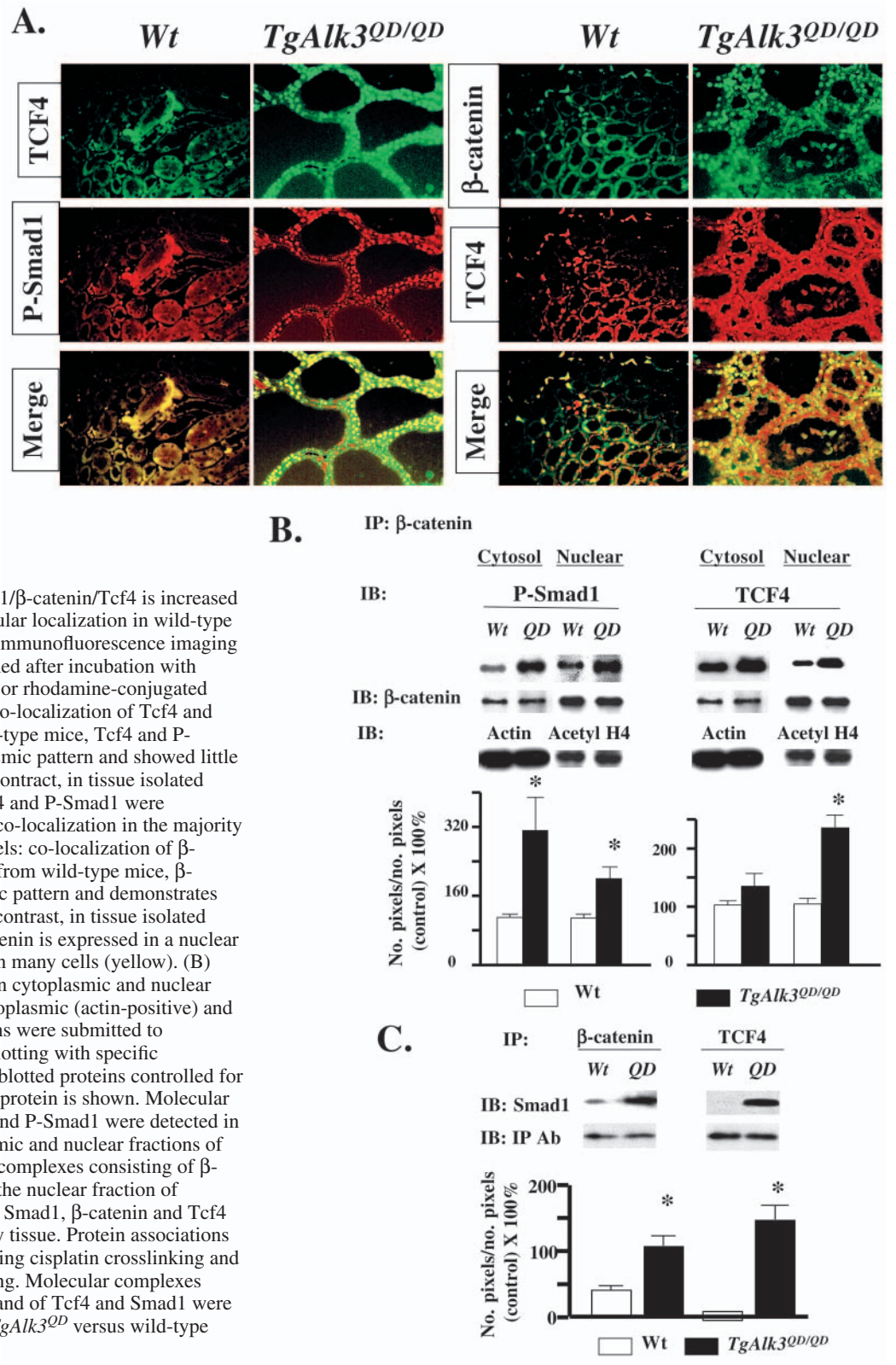

Fig. 2. Nuclear association of Smad1/β-catenin/Tcf4 is increased in *TgAlk3*^{QD} kidney tissue. (A) Cellular localization in wild-type and cystic *TgAlk3*^{QD} kidney tissue. Immunofluorescence imaging of 4 μm tissue sections was performed after incubation with primary antibodies and fluorescein- or rhodamine-conjugated secondary antibodies. Left panels: co-localization of Tcf4 and Smad1. In tissue isolated from wild-type mice, Tcf4 and P-Smad1 were expressed in a cytoplasmic pattern and showed little co-localization (merge image). By contract, in tissue isolated from *TgAlk3*^{QD} mouse kidneys, Tcf4 and P-Smad1 were expressed in a nuclear pattern with co-localization in the majority of imaged cells (yellow). Right panels: co-localization of β-catenin and Tcf4. In tissue isolated from wild-type mice, β-catenin is expressed in a cytoplasmic pattern and demonstrates little co-localization with Tcf4. By contrast, in tissue isolated from *TgAlk3*^{QD} mouse kidney, β-catenin is expressed in a nuclear pattern and co-localizes with Tcf4 in many cells (yellow). (B) Detection of molecular complexes in cytoplasmic and nuclear fractions. Proteins derived from cytoplasmic (actin-positive) and nuclear (acetyl H4-positive) fractions were submitted to immunoprecipitation and immunoblotting with specific antibodies. Quantitation of immunoblotted proteins controlled for the quantity of immunoprecipitated protein is shown. Molecular complexes consisting of β-catenin and P-Smad1 were detected in increased amounts in both cytoplasmic and nuclear fractions of *TgAlk3*^{QD} kidney tissue. Molecular complexes consisting of β-catenin and Tcf4 were increased in the nuclear fraction of *TgAlk3*^{QD} tissue. (C) Association of Smad1, β-catenin and Tcf4 with chromatin isolated from kidney tissue. Protein associations with nuclear DNA were assessed using cisplatin crosslinking and immunoprecipitation/immunoblotting. Molecular complexes consisting of β-catenin and Smad1 and of Tcf4 and Smad1 were detected in increased quantities in *TgAlk3*^{QD} versus wild-type kidney tissues.

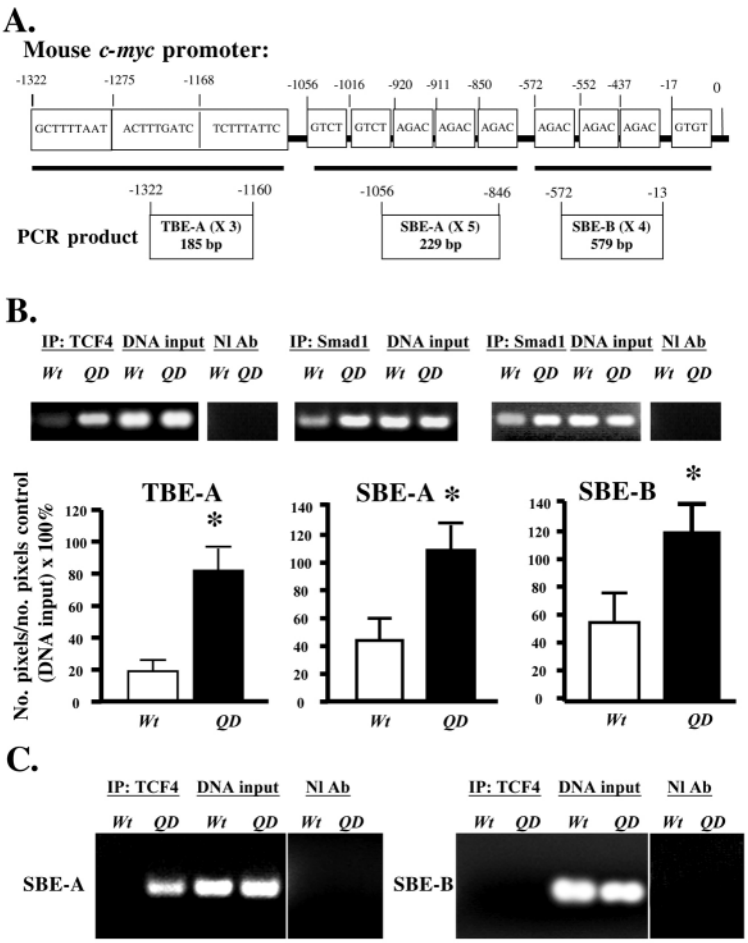

Fig. 3. Associations of Smad1, β-catenin and Tcf4 with the Myc promoter are enhanced in *TgAlk3*^{QD} kidney tissue. (A) Schematic representation of mouse Myc promoter. The 1409 nucleotide region upstream of the transcription start site is organized into Tcf-binding element (TBE), TBE-A, consisting of three Tcf-binding consensus sequences, an adjacent Smad-binding element (SBE), SBE-A, consisting of five Smad-binding consensus sequences, and a second SBE, SBE-B, consisting of four Smad-binding consensus sequences. (B) Results of ChIP. DNA amplified using region-specific primers is shown above graphs demonstrating quantitation of corresponding amplified DNA controlled for the amount of input DNA. Antibody controls using non-immune sera are shown for each ChIP. Left panel: ChIP of TBE-A using anti-Tcf4 antibody showing increased association of Tcf4 with TBE-A in *TgAlk3*^{QD} kidney tissues versus wild type. Middle and right panels: ChIP of SBE-A and SBE-B using anti-Smad1 antibody showing increased association of Smad1 with SBE-A and SBE-B in *TgAlk3*^{QD} kidney tissue. (C, left panels) ChIP of SBE-A using anti-Tcf4 antibody showing association of Tcf4 with SBE-A in *TgAlk3*^{QD} kidney tissue but not in wild-type tissue. (C, right panels) ChIP of SBE-B using anti-Tcf4 antibody. No association of Tcf4 with SBE-B was detected in either wild-type or *TgAlk3*^{QD} kidney tissue.

either wild-type or *TgAlk3*^{QD} tissue. However, the intensity of the retarded band was greater with *TgAlk3*^{QD} nuclear extract consistent with increased binding of the oligo-duplex by components of the extract. Addition of anti-Tcf4 antibody to nuclear extract generated from *TgAlk3*^{QD} or wild-type tissue generated a marked supershift of the oligo-duplex, indicating binding of the oligo-duplex by Tcf4 resident in the nuclei of *TgAlk3*^{QD} and wild-type tissues. However, the greater intensity of the supershifted band indicated higher levels of Tcf4 in *TgAlk3*^{QD} extracts. Moreover, the mobility of the supershifted band was slower in *TgAlk3*^{QD} samples, suggesting that the molecular composition of the Tcf4-containing molecular complexes differs between *TgAlk3*^{QD} and wild-type tissues. Addition of anti-β-catenin antibody to nuclear extract also caused a supershift with greater intensity of the supershifted band in *TgAlk3*^{QD} extracts, consistent with known interactions between β-catenin and Tcfs. The mobility of the supershifted bands in *TgAlk3*^{QD} and wild-type tissues differed as observed in samples treated with anti-Tcf4 antibody. Addition of anti-Smad1 antibody also generated a supershift. However, this effect was observed only in dysplastic kidney tissue (Fig. 4A, left panel). The mobility of the supershifted band was identical to that observed in *TgAlk3*^{QD} nuclear lysates treated with anti-Tcf4 antibody or anti-β-catenin antibody. These results suggest that the molecular complex that associates with TBE in *TgAlk3*^{QD} nuclei consists of Smad1, β-catenin and Tcf4, while that in wild-type nuclei does not contain Smad1. The requirement for Tcf consensus sequences in these interactions was shown by lack of binding by nuclear extracts in experiments in which a mutant TBE oligo-duplex was substituted for the corresponding wild-type oligo-duplex (Fig. 4A, right panel). The specificity of the interaction between oligo-duplex and nuclear lysates was demonstrated by loss of the shifted band after addition of unlabeled probe (Fig. 4B). The specificity of protein-specific antisera in generating supershifted bands was shown by the absence of these bands when non-immune serum was substituted (Fig. 4C). Taken together, these results provide further evidence favoring the existence of a Smad1/β-catenin/Tcf4 molecular complex associated with TBE-A in dysplastic renal tissue.

We used a similar approach to examine the association of Tcf4 and β-catenin with Smad1 at SBE-A. The migration of a radiolabeled oligo-duplex encoding a 46 nucleotide sequence within SBE-A was retarded by nuclear extract prepared from either wild-type or *TgAlk3*^{QD} tissue. Addition of anti-Smad1 antibody to nuclear extract generated from *TgAlk3*^{QD} or wild-type tissue generated a marked supershift of the oligo-duplex, indicating binding of the oligo-duplex by Smad1 resident in the nuclei of both *TgAlk3*^{QD} and wild-type tissues. However, the intensity of the supershifted band was much greater for *TgAlk3*^{QD} extracts, indicating larger amounts of Smad1 in *TgAlk3*^{QD} nuclei. Moreover, the mobility of the supershifted band was slower in *TgAlk3*^{QD} samples, suggesting that the molecular composition of the Smad1-containing molecular complexes is different in *TgAlk3*^{QD} versus wild-type tissues. Addition of anti-β-catenin antibody generated bands of similar mobility to those generated after addition of anti-Smad1 antibody. Remarkably, addition of anti-Tcf4 antibody generated a supershifted band only in *TgAlk3*^{QD} nuclear extracts. Together, these results suggest that the molecular complex that associates with SBE-A in *TgAlk3*^{QD} nuclear lysates consists of Smad1, Tcf4 and β-catenin, while the molecular complex that associates with SBE-A in control tissues consists only of Smad1 and β-catenin (Fig. 4D, left

panel). The requirement for Smad-binding consensus sequences in these interactions was shown by lack of binding by nuclear extracts in experiments in which a mutant SBE oligo-duplex was substituted for the corresponding wild-type oligo-duplex (Fig. 4D, right panel). The specificity of the interaction between oligo-duplex and nuclear lysates was demonstrated by loss of the shifted band after addition of unlabeled probe (Fig. 4E). The specificity of protein-specific antisera in generating supershifted bands was shown by the

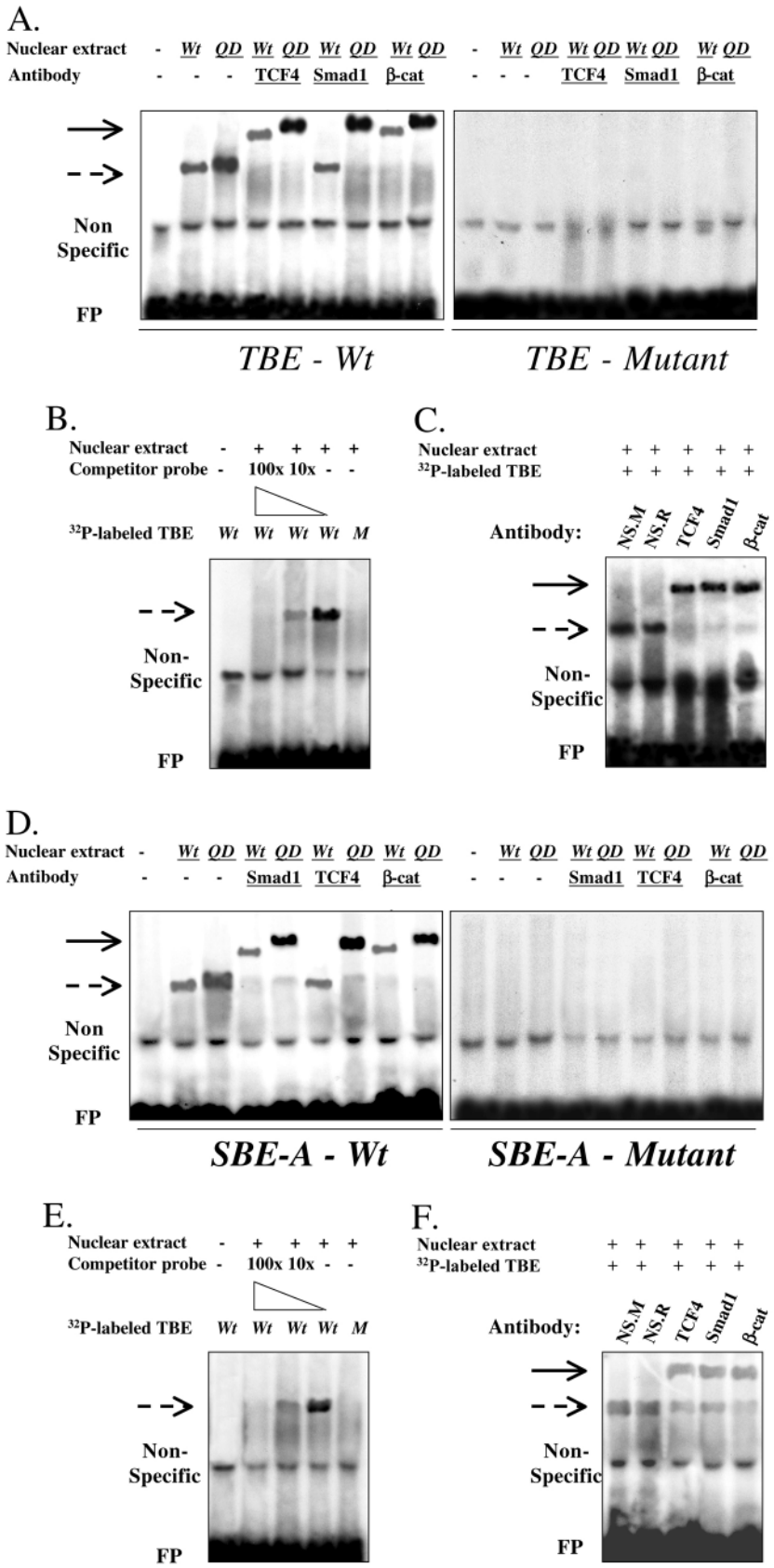

Fig. 4. Association of Smad1/Tcf4/β-catenin molecular complexes with oligo-duplexes encoding either TBE-A or SBE-A. EMSA showing inhibition of migration generated by incubating nuclear extracts isolated from wild-type or *TgAlk3*^{QD} *(QD)* kidney tissue with ^{32}P-labeled oligo-duplexes corresponding to wild-type and mutant consensus binding regions within TBE-A and SBE-A (broken arrow). Unbroken arrows mark enhanced inhibition of migration associated with addition of specific antibodies. Free probe (FP) is observed at the lower end of each autoradiogram. (A) Left panel: migration of ^{32}P-labeled oligo-duplex, TBE-A, was retarded by addition of nuclear extract (broken arrow). The amount of oligo-duplex bound by extract from *QD* was greater than that from wild type. Addition of specific antibody caused a further migratory retardation (unbroken arrow). Association of Tcf4 was detected in both wild type and *QD* but at much higher levels in *QD*. Association of β-catenin was detected at low levels in wild type and at much higher levels in *QD*. Association of Smad1 with TBE-A sequences was observed only in *QD*. The mobility of the supershifted band was greater in *QD* lysates compared with wild-type lysates. Right panel: specificity of TBE-A is demonstrated by failure to detect any specific retardation using a mutant version of TBE-A. (B) The specificity of DNA-protein interactions (broken arrow) is shown by progressive diminution of binding in the presence of tenfold and 100-fold excess of unlabeled oligo-duplex. (C) The specificity of antibody-mediated supershifts (unbroken arrow) is shown by the absence of a supershift in the presence of non-immune mouse or rat antisera. (D) Left panel: migration of ^{32}P-labeled oligo-duplex, SBE-A, was retarded by addition of nuclear extract (broken arrow). The amount of oligo-duplex bound by extract from *QD* was greater than that from wild type. Addition of specific antibody caused a further migratory retardation (unbroken arrow). Association of Smad1 with SBE-A was detected in both wild type and *QD* with greater amounts detected in *QD*. Association of β-catenin was detected in wild type and at much higher levels in *QD*. Association of Tcf4 was detected only in *QD*. The mobility of the supershifted band was greater in *QD* lysates compared with wild-type lysates. Right panel: specificity of SBE-A is demonstrated by failure to detect any specific retardation using a mutant version of SBE-A. (E) The specificity of DNA-protein interactions (broken arrow) is shown by progressive diminution of binding in the presence of tenfold and 100-fold excess of unlabeled oligo-duplex. (F) The specificity of antibody-mediated supershifts (unbroken arrow) is shown by the absence of a supershift in the presence of non-immune mouse or rat antisera.

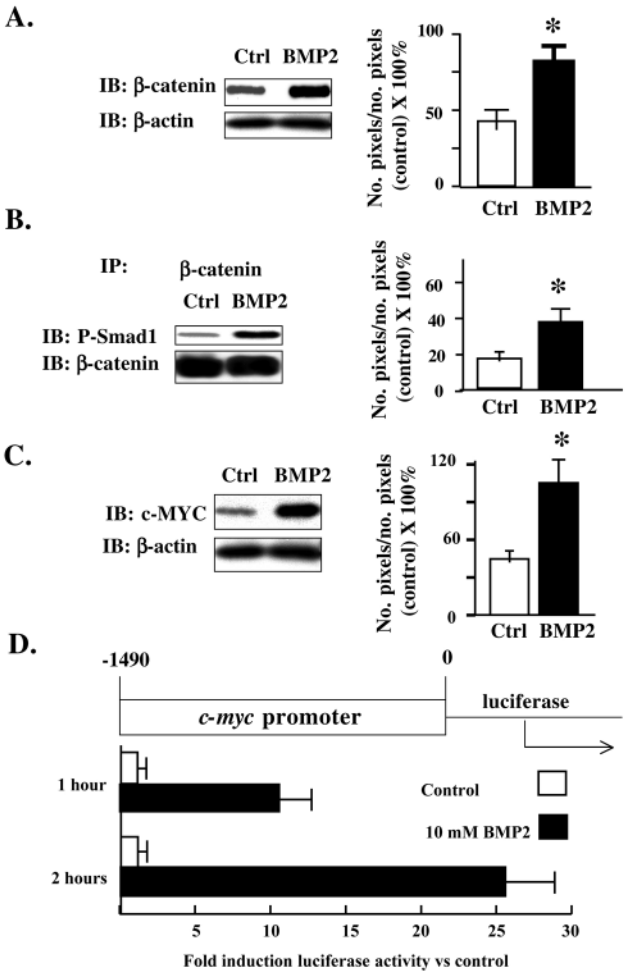

Fig. 5. Treatment of mIMCD-3 cells with Bmp2 increases β-catenin/P-Smad1 molecular complexes and Myc expression. Immunoblots and quantitation are shown on the left and right panels, respectively. Treatment with recombinant 10 nM Bmp2 increased intracellular levels of β-catenin 1.9-fold (A), β-catenin/P-Smad1 molecular complexes 2.3-fold (B) and Myc 2.4-fold (C). (D) Bmp2 treatment of mIMCD-3 cells transfected with a plasmid encoding the Myc promoter (–1490 to –1) upstream of luciferase increased luciferase activity 10-fold by 1 hour and 26-fold by 2 hours after addition of Bmp2.

absence of these bands when non-immune serum was substituted (Fig. 4F). Taken together, these results provide further evidence favoring the existence of a Smad1/β-catenin/Tcf4 molecular complex associated with SBE-A in dysplastic renal tissue.

Bmp2 induces formation of β-catenin/P-Smad1 molecular complexes and Myc expression in collecting duct cells in vitro

We developed an in vitro model aimed at investigating the functional consequences of Alk3-dependent Smad1/β-catenin/Tcf4 interactions with the Myc promoter. Previously, we have demonstrated that treatment of inner medullary collecting duct (mIMCD-3) cells with Bmp2 activates Alk3 and Smad1 (Gupta et al., 1999). Further investigation of Bmp2-mediated effects demonstrated simultaneous increases in the cellular levels of β-catenin and P-Smad1/β-catenin molecular complexes 1.9-fold and 2.3-fold, respectively (Fig. 5A,B). These increases were associated with a 2.4-fold increase in Myc (Fig. 5C). Moreover, Bmp2 treatment of mIMCD-3 cells transfected with a plasmid encoding luciferase under the control of the 1490-nucleotide segment of the Myc promoter increased luciferase activity by as much as 26-fold after addition of Bmp2 (Fig. 5D). Together, these observations provided a basis for testing the functional consequences of Smad/β-catenin interactions on Myc promoter function.

Smad1, β-catenin and Tcf4 cooperate to control Myc transcription

We used RNAi to determine the effect of Tcf4, β-catenin or Smad1 on Myc transcription. Plasmid-mediated RNAi decreased intracellular levels of Tcf4, β-catenin or Smad1 by 85%, 75% and 92%, respectively, in mIMCD-3 cells (data not shown). The decrease in Tcf4 or β-catenin decreased the basal levels of Myc mRNA and protein to a similar degree and totally abrogated the ~30% increase in Myc mRNA and protein expression observed after treatment with Bmp2 (Fig. 6A,B). By contrast, knock-down of Smad1 had no significant effect on basal amounts of Myc. Remarkably, however, similar to Tcf4 and β-catenin, RNAi versus Smad1 eliminated the stimulatory response to Bmp2 (Fig. 6A,B). Thus, these results suggested a stimulatory role for each of Tcf4, β-catenin and Smad1 in Myc transcription and provided a basis for using RNAi to investigate the role of these effectors in controlling the Myc promoter segment shown in our preceding experiments to associate with these proteins.

We investigated the effect of RNAi-mediated knock-down on the basal and Bmp2-stimulated activity of the 1490 nucleotide Myc promoter. Reduction of Tcf4 significantly reduced basal promoter activity compared with control (empty pSUPER plasmid) and totally abrogated the 20-fold increase in luciferase activity observed with Bmp2 treatment. By contrast, reduction of β-catenin did not affect basal promoter activity but did totally inhibit the stimulatory response to Bmp2. Similar to β-catenin, reduction in Smad1 exerted no significant effect on basal promoter activity but, by contrast, permitted only an attenuated (fourfold) response to Bmp2 (Fig. 6C). These results demonstrate that Tcf4 is required for basal function of Myc. Both Tcf4 and β-catenin are required for Bmp2-mediated stimulation and Smad1 is required for a full transcriptional response to Bmp2.

Our results indicate that Smad1 is a positive regulator of Myc transcription in the context of Tcf4 and β-catenin. As Smads have been shown previously to inhibit Myc transcription (Yagi et al., 2002), we investigated the function of SBE-A to determine whether it is a positive or negative regulator of Myc. Using site-directed mutagenesis, we introduced nucleotide substitutions into the Tcf-A or SBE-A regions of the Myc promoter and then determined the function of the 1490 nucleotide promoter segment in mIMCD-3 cells in the presence or absence of Bmp2. Mutagenesis of a single Tcf consensus binding site (AT to GC) within Tcf-A decreased the basal activity of the promoter and largely inhibited Bmp2-dependent promoter activity, consistent with the functions for Tcf and β-catenin elucidated using RNAi. Mutagenesis of SBE-A via nucleotide substitutions in two distinct consensus sequences significantly increased basal Myc promoter activity,

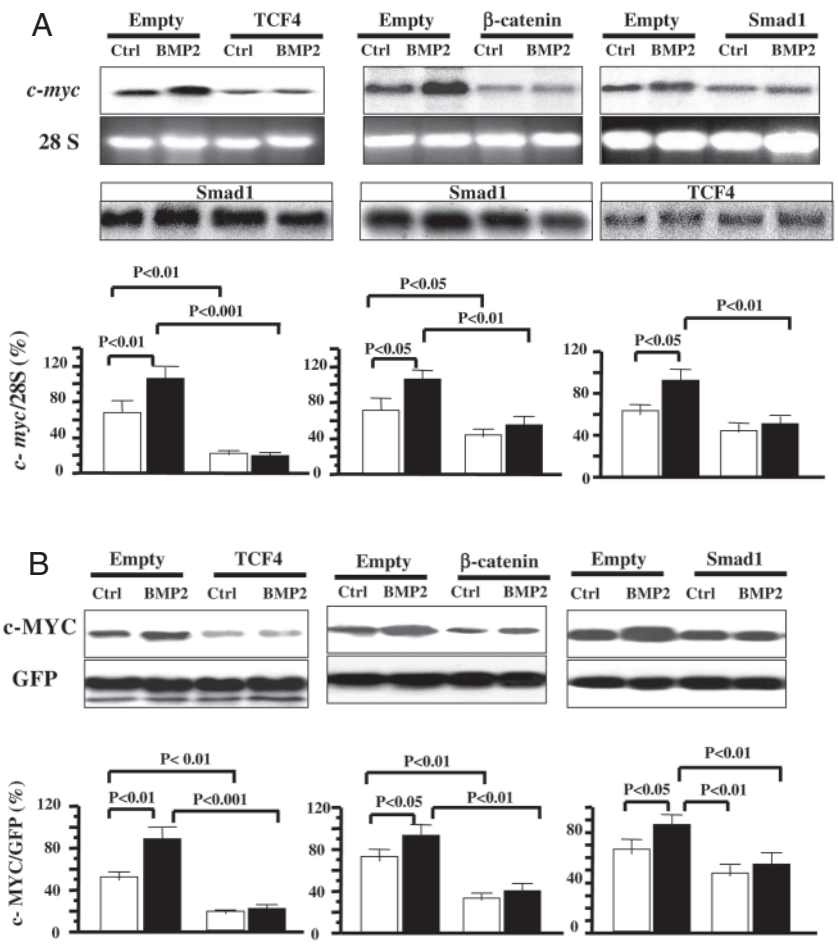

suggesting that these sequences act to inhibit Myc during a state in which Tcf4/β-catenin/Smad1 complex formation is not stimulated. By contrast, in a condition in which this molecular complex is induced (Bmp2 treatment), an intact SBE-A was required for a full stimulatory response (Fig. 6D). These results suggest that Smad1-SBE-A function is converted from an inhibitory to a stimulatory function in a state during which interactions between Smad1 and β-catenin/Tcf4 occur.

Discussion

The *TgAlk3^{QD}* model of renal medullary dysplasia

We recently described the *TgAlk3^{QD}* model of renal dysplasia. The kidney histopathology in these mice is characteristic of types of renal dysplasia in which tissue maldevelopment does not involve all components of the kidney but, rather, is restricted to one or more tissue elements (Piscione and Rosenblum, 1999). In the *TgAlk3^{QD}* model, nephrogenesis is intact albeit quantitatively deficient, and the collecting duct lineage is characterized by a decreased number of tubules and cystic degeneration of these tubules. We have proposed a two-phase model accounting for the genesis of these collecting duct abnormalities (Hu et al., 2003). This model suggests that decreased branching of the ureteric bud due to increased Alk3 and Smad activity (Phase I)

Fig. 6. Tcf4, β-catenin and Smad1 positively regulate Myc. (A,B) Effect of RNAi-mediated decrease in Tcf4, β-catenin or Smad1 on endogenous Myc mRNA and protein in mIMCD-3 cells. In control cells transfected with an empty plasmid, Bmp2 significantly increased levels of endogenous Myc mRNA and protein. (A,B) Knock-down of Tcf4 or β-catenin decreased basal levels of Myc mRNA and protein, and totally blocked Bmp2-mediated increases in these species. Knock-down of Tcf4 exerted a larger inhibitory effect on basal levels. Knock-down of Smad1 did not exert a significant effect on basal mRNA and protein levels but did partially block the Bmp2 mediated increase observed in controls. (C) Effect of RNAi-mediated decrease in Tcf4, β-catenin or Smad1 on luciferase activity downstream of the –1490 to –1 segment of the Myc promoter. In controls transfected with an empty RNAi-inducing plasmid, Bmp2 markedly induced luciferase activity. Knock-down of Tcf4 significantly decreased basal luciferase activity and totally abrogated the Bmp2-dependent increase in luciferase activity. Knock-down of either β-catenin or Smad1 exerted no significant effect on luciferase activity under basal conditions. Knock-down of β-catenin blocked the Bmp2-dependent increase. By contrast, the response to Bmp2 was limited to a partial but significant response in cells with a quantitatively similar reduction in Smad1 levels. (D) Role of TBE-A and SBE-A in Bmp2-dependent induction of Myc luciferase. mIMCD-3 cells were transfected with plasmid DNA encoding luciferase downstream of either wild-type or mutant forms of the Myc promoter (–1490 to –1). Under basal conditions (no Bmp2 treatment), luciferase activity was significantly decreased under the control of the mutant TBE-A and significantly increased downstream of the mutant SBE-A. Mutant TBE-A significantly decreased Bmp2-dependent induction of luciferase activity. Mutant SBE-A also decreased Bmp2-dependent induction of luciferase activity but not to the same extent as mutant TBE-A.

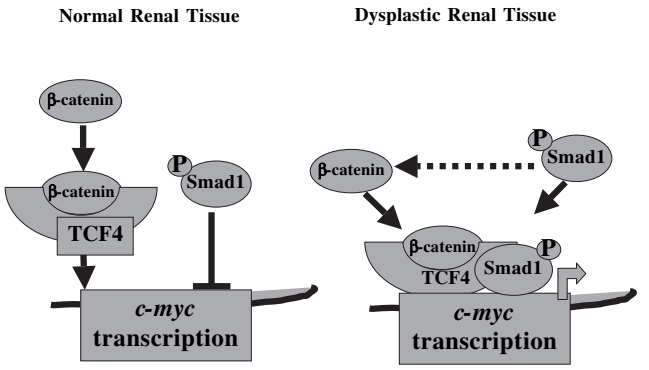

Fig. 7. Model of Smad/β-catenin signaling in normal and dysplastic renal tissues. In the absence of Bmp-stimulated Smad1/β-catenin interactions, Myc expression is inhibited by Smad1 bound to Smad-binding regions. By contrast, in dysplastic tissue, formation of Smad1/β-catenin/Tcf4 molecular complexes stimulates *Myc* transcription via mechanisms to be defined.

leads to sustained elevation in the levels of intracellular β-catenin and formation of Smad1/β-catenin molecular complexes associated with collecting duct cell dedifferentiation and cystic malformation of these elements (Phase 2). Our finding that Smad1 and β-catenin are misexpressed in cystic tubules resident in human fetal dysplastic kidneys strongly suggests that signaling by Smads and β-catenin is pathogenic during the genesis of renal dysplasia.

The data described in this paper provide further insight into how Smad1/β-catenin interactions may control epithelial dedifferentiation and cyst formation focusing on Myc, a paradigm for genes that control these pathological processes. Myc is involved in a wide range of cellular processes, including proliferation, differentiation and tumorigenesis (Grandori et al., 2000). Of relevance to the $TgAlk3^{QD}$ model, the general observation that Myc expression strongly correlates with growth and proliferation is consistent with our finding of Myc expression in epithelia marked by an increased rate of proliferation (Hu et al., 2003). Our finding that Myc expression is associated with loss of epithelial differentiation markers is in agreement with previous reports showing that Myc overexpression inhibits terminal differentiation in a wide variety of cell types. The relevance of our observations regarding Myc is further supported by the recognition that Myc is misexpressed in collecting duct cells in murine recessive polycystic kidney disease (PKD) (Cowley et al., 1987), that overexpression of Myc induces PKD in mice (Trudel et al., 1998) and that antisense-mediated downregulation of Myc ameliorates PKD in mice (Ricker et al., 2002). Thus, investigation of mechanisms that control Myc gene regulation is fundamental to understanding tissue maldevelopment and epithelial cell differentiation.

Control of Myc transcription by Smad1, β-catenin and Tcf4

The recognition that the Myc promoter contains Smad-binding elements as well as Tcf finding elements (Yagi et al., 2002) led us to investigate the nature of Smad/β-catenin interactions at the level of gene transcription. Several of our observations suggested that these interactions are, at the very least enhanced, if not induced, in dysplastic $TgAlk3^{QD}$ compared with wild-type tissue. First, molecular complexes consisting of Smad1, β-catenin and Tcf4 are detectable in significantly higher amounts in $TgAlk3^{QD}$ kidney tissue compared with wild-type tissue. Second, interactions between Tcf4 and a Smad-binding element contiguous with a Tcf-binding element in the Myc promoter were observed only in dysplastic tissue. Third, interaction between Smad1, β-catenin and Tcf4 with Smad- or Tcf-binding sequences were observed at high levels in nuclear lysates generated from dysplastic renal tissue but were not detectable in wild-type renal tissues. Our studies in a collecting duct cell model of Bmp-dependent Smad1/β-catenin interactions extend these observations at a functional level. Using RNAi and site-directed mutagenesis, we demonstrate that not only Tcf4 and β-catenin but also Smad1 are required for Bmp-dependent stimulation of Myc. Consistent with these results, examination of the function of the Smad-binding region adjacent to the Tcf-binding region revealed that these sequences subserve a positive role in the context of Bmp-stimulated Myc expression but an inhibitory function in the absence of these conditions.

Our studies expand the breadth of signaling interactions between the Smad and β-catenin pathways previously described. Molecular interactions between Bmp and Tcf signaling effectors have been described during the control of *Msx2* promoter activity in mouse embryonic stem cells (Hussein et al., 2003). The *Msx2* promoter contains two SBEs and two TBEs upstream of the SBEs. As expected, Bmp2 stimulation of *Msx2* is dependent on the SBEs. However, rather surprisingly, Bmp2 stimulatory activity is also dependent on the TBEs. Consistent with this finding is the recognition that Bmp2 induces recruitment of LEF1/Tcf to the promoter, association of Lef1/Tcf with the SBE and association of Smad1 with the TBE. Molecular interactions between Smad and β-catenin effectors during normal embryogenesis have been observed between Smad4 and Lef1/Tcf and between Smad4 and β-catenin in *Xenopus*, specifically involving cooperative interactions between Smad4 and Lef1/Tcf at the *Xtwn* promoter (Nishita et al., 2000). The nature of these interactions has been further elucidated in genetic cell models. The Xtwn promoter contains a SBE and TBE within a 322 nucleotide region. Lef1/Tcf stimulates transcription; TGFβ, alone, does not stimulate. However, TGFβ stimulates in the presence of Lef1/Tcf and induces binding of Smad3/Lef1 molecular complexes to the Xtwn promoter. Indeed, the effect of Lef1/Tcf is enhanced in the presence of Smad3 and mutagenesis of the SBE partially abrogates Smad-dependent enhancement of Lef1/Tcf stimulation (Labbe et al., 2000). Our results in the $TgAlk3^{QD}$ model are consistent with these reports, demonstrating the conversion of a Bmp-dependent inhibitory function to a stimulatory effect that enhances Tcf signaling in a manner that is associated with Smad/Tcf complexes and Tcf/SBE interaction and is dependent on the SBE. Thus, our work demonstrates the relevance of Smad/Tcf interactions to mammalian tissue morphogenesis in health and disease.

Our results in the $TgAlk3^{QD}$ model reveal a functional role for β-catenin in Smad/Tcf interactions, a finding that is different than observations made during the analysis of *Xtwn* and *Msx2*. Constitutive action of Alk3 increases β-catenin levels and associations between β-catenin, Tcf and P-Smad1 in

the nucleus. β-catenin is detected together with Smad1 and Tcf4 in nuclear extracts that bind to sequences within SBE-A and TBE-A, suggesting a role for β-catenin in transcription. Such a function for β-catenin is further suggested by our finding that Bmp-dependent induction of Myc is abrogated when intracellular levels of β-catenin are lowered. Thus, in contrast to embryonic stem cells (Hussein et al., 2003), in dysplastic kidney tissue β-catenin may serve to mediate Smad/Tcf protein interactions via its property of binding to both Smads and Tcfs simultaneously via separate domains (Labbe et al., 2000).

Model of Smad and β-catenin/Tcf signaling in normal and dysplastic kidney tissue

Our analysis of Smad1, β-catenin and Tcf4 signaling in the *TgAlk3^{QD}* model of renal dysplasia suggests a model of Smad/β-catenin signaling in normal and dysplastic renal tissues (Fig. 7). This model suggests that in the absence of Bmp-stimulated Smad1/β-catenin interactions, Myc expression is inhibited by Smad1 bound to Smad-binding regions. We have identified two regions containing a minimum of seven Smad-binding elements within the first 1400 nucleotides upstream of the Myc transcription start site. It is possible that other Smad-binding elements exist within other regulatory regions. In a manner elucidated for TGFβ-dependent repression of Myc, it is likely that Smad1 acts in concert with other transcription factors to inhibit Myc (Chen et al., 2002; Frederick et al., 2004). Our model further suggests that in pathological states associated with recruitment of Smad1 to molecular complexes consisting of β-catenin and Tcf4, the Smad1-containing complex acts to stimulate. The mechanisms that control this switch in Smad activity remain to be discovered but probably involve recruitment of other transcription factors that bind to Smad proteins and control transcription via direct or indirect mechanisms. Further elucidation of these mechanisms will provide a basis for inhibiting pathogenic signaling interactions in dysplastic tissue.

The authors thank Drs B. Alman, J. Ellis and H. Lipshitz for helpful discussion and Drs. S. El-Dahr and Z. Saifudeen for excellent advice regarding ChIP. This research was supported by a grant from the Canadian Institutes of Health Research (to N.D.R.).

References

Brummelkamp, T. R., Bernards, R. and Agami, R. (2002). A system for stable expression of short interfering RNAs in mammalian cells. *Science* **296**, 550-553.

Chen, C. R., Kang, Y., Siegel, P. M. and Massague, J. (2002). E2F4/5 and p107 as Smad cofactors linking the TGFbeta receptor to c-myc repression. *Cell* **110**, 19-32.

Chichiarelli, S., Coppari, S., Turano, C., Eufemi, M., Altieri, F. and Ferraro, A. (2002). Immunoprecipitation of DNA-protein complexes cross-linked by cis-Diamminedichloroplatinum. *Anal. Biochem.* **302**, 224-229.

Cowley, B. D., Jr, Smardo, F. L., Jr, Grantham, J. J. and Calvet, J. P. (1987). Elevated c-myc protooncogene expression in autosomal recessive polycystic kidney disease. *Proc. Natl. Acad. Sci. USA* **84**, 8394-8398.

Dewulf, N., Verschueren, K., Lonnoy, O., Morén, A., Grimsby, S., Vande Spiegle, K., Miyazono, K., Huylebroeck, D. and Ten Dijke, P. (1995). Distinct spatial and temporal expression patterns of two type 1 receptors for bone morphogenetic proteins during mouse embryogenesis. *Endocrinology* **136**, 2652-2663.

Frederick, J. P., Liberati, N. T., Waddell, D. S., Shi, Y. and Wang, X. F. (2004). Transforming growth factor beta-mediated transcriptional repression of c-myc is dependent on direct binding of Smad3 to a novel repressive Smad binding element. *Mol. Cell Biol.* **24**, 2546-2559.

Grandori, C., Cowley, S. M., James, L. P. and Eisenman, R. N. (2000). The Myc/Max/Mad network and the transcriptional control of cell behavior. *Annu. Rev. Cell Dev. Biol.* **16**, 653-699.

Grunstein, M. (1997). Histone acetylation in chromatin structure and transcription. *Nature* **389**, 349-352.

Gupta, I. R., Piscione, T. D., Grisaru, S., Phan, T., Macias-Silva, M., Zhou, X., Whiteside, C., Wrana, J. L. and Rosenblum, N. D. (1999). Protein Kinase A is a negative regulator of renal branching morphogenesis and modulates inhibitory and stimulatory bone morphogenetic proteins. *J. Biol. Chem.* **274**, 26305-26314.

He, T. C., Sparks, A. B., Rago, C., Hermeking, H., Zawel, L., da Costa, L. T., Morin, P. J., Vogelstein, B. and Kinzler, K. W. (1998). Identification of Myc as a target of the APC pathway. *Science* **281**, 1509-1512.

Hu, M. C., Piscione, T. D. and Rosenblum, N. D. (2003). Elevated Smad1/β-catenin molecular complexes and renal medullary cystic dysplasia in ALK3 transgenic mice. *Development* **130**, 2753-2766.

Hussein, S. M., Duff, E. K. and Sirard, C. (2003). Smad4 and beta-catenin co-activators functionally interact with lymphoid-enhancing factor to regulate graded expression of Msx2. *J. Biol. Chem.* **278**, 48805-48814.

Labbe, E., Letamendia, A. and Attisano, L. (2000). Association of Smads with lymphoid enhancer binding factor 1/T cell-specific factor mediates cooperative signaling by the transforming growth factor-ß and Wnt pathways. *Proc. Natl. Acad. Sci. USA* **97**, 8358-8363.

Miyazaki, Y., Oshima, K., Fogo, A., Hogan, B. L. and Ichikawa, I. (2000). Bone morphogenetic protein 4 regulates the budding site and elongation of the mouse ureter. *J. Clin. Invest.* **105**, 863-873.

Neu, A. M., Ho, P. L., McDonald, R. A. and Warady, B. A. (2002). Chronic dialysis in children and adolescents. The 2001 NAPRTCS Annual Report. *Pediatr. Nephrol.* **17**, 656-663.

Nishita, M., Hashimoto, M. K., Ogata, S., Laurent, M. N., Ueno, N., Shibuya, H. and Cho, K. W. (2000). Interaction between Wnt and TGF-beta signalling pathways during formation of Spemann's organizer. *Nature* **403**, 781-785.

Piscione, T. D. and Rosenblum, N. D. (1999). The malformed kidney: disruption of glomerular and tubular development. *Clin. Genet.* **56**, 343-358.

Piscione, T. D. and Rosenblum, N. D. (2002). The molecular control of renal branching morphogenesis: current knowledge and emerging insights. *Differentiation* **70**, 227-246.

Piscione, T. D., Yager, T. D., Gupta, I. R., Grinfeld, B., Pei, Y., Attisano, L., Wrana, J. L. and Rosenblum, N. D. (1997). BMP-2 and OP-1 exert direct and opposite effects on renal branching morphogenesis. *Am. J. Physiol.* **273**, F961-F975.

Pohl, M., Bhatnagar, V., Mendoza, S. A. and Nigam, S. K. (2002). Toward an etiological classification of developmental disorders of the kidney and upper urinary tract. *Kidney Int.* **61**, 10-19.

Ricker, J. L., Mata, J. E., Iversen, P. L. and Gattone, V. H. (2002). c-myc antisense oligonucleotide treatment ameliorates murine ARPKD. *Kidney Int. Suppl.* **61**, 125-131.

Saifudeen, Z., Marks, J., Du, H. and El-Dahr, S. S. (2002). Spatial repression of PCNA by p53 during kidney development. *Am. J. Physiol. Renal. Physiol.* **283**, F727-F733.

Saxen, L. (1987). *Organogenesis of the Kidney*. Cambridge, UK: Cambridge University Press.

Trudel, M., Barisoni, L., Lanoix, J. and D'Agati, V. (1998). Polycystic kidney disease in SBM transgenic mice: role of c-myc in disease induction and progression. *Am. J. Pathol.* **152**, 219-229.

Weinmann, A. S., Bartley, S. M., Zhang, T., Zhang, M. Q. and Farnham, P. J. (2001). Use of chromatin immunoprecipitation to clone novel E2F target promoters. *Mol. Cell Biol.* **21**, 6820-6832.

Weinmann, A. S. and Farnham, P. J. (2002). Identification of unknown target genes of human transcription factors using chromatin immunoprecipitation. *Methods* **26**, 37-47.

Yagi, K., Furuhashi, M., Aoki, H., Goto, D., Kuwano, H., Sugamura, K., Miyazono, K. and Kato, M. (2002). c-myc is a downstream target of the Smad pathway. *J. Biol. Chem.* **277**, 854-861.